Composite Structures 92 (2010) 1786–1792

Contents lists available at ScienceDirect

Composite Structures

journal homepage: www.elsevier.com/locate/compstruct

A wavelet collocation method for the static analysis of sandwich plates using a layerwise theory

Luís M.S. Castro [a,*], A.J.M. Ferreira [b], Silvia Bertoluzza [c], R.C. Batra [d], J.N. Reddy [e]

[a] Departamento de Engenharia Civil e Arquitectura, IST-UTL, Avenida Rovisco Pais, 1049-001 Lisboa, Portugal
[b] Departamento de Engenharia Mecânica, Faculdade de Engenharia da Universidade do Porto, Rua Dr. Roberto Frias, 4200-465 Porto, Portugal
[c] Istituto di Matematica Applicata e Tecnologie Informatiche del C.N.R., via Ferrata, 1, 27100 Pavia, Italy
[d] Department of Engineering Science and Mechanics, MC0219, Virginia Polytechnic Institute and State University, Blacksburg, VA 24061, USA
[e] Department of Mechanical Engineering, Texas A&M University College Station, TX 777843-3123, USA

ARTICLE INFO

Article history:
Available online 6 February 2010

Keywords:
Sandiwch plates
Collocation methods
Wavelets
Layerwise theory
Static analysis

ABSTRACT

A study of bending deformations of sandwich plates using a layerwise theory of laminated or sandwich plates is presented. The analysis is based on a wavelet collocation technique to produce highly accurate results. Numerical results for symmetric laminated composite and sandwich plates are presented and discussed.

1. Introduction

Bending and free vibration of shear-flexible plates by numerical techniques was performed by [1–3] using the differential quadrature method. In [4–7] the finite element method was used with success. More recently the analysis of isotropic and laminated plates by Kansa's non-symmetric radial basis function collocation method was performed by Ferreira and colleagues [8–16].

This paper deals with the bending analysis of sandwich plates by a wavelet collocation method [17,18]. A layerwise theory is used to model the kinematics of the laminated plates. Although in the present study we restrict the analysis to sandwich plates, the method can be easily applied to isotropic as well as more complicated plate bending problems, such as piezolaminates, or laminates with distributed actuators.

The method employed for the numerical solution is a collocation method based on Deslaurier–Dubuc interpolating basis in hierarchical form [19], which is the first necessary step towards the application to this class of problems of the adaptive wavelet collocation method introduced in [17,20]. This collocation algorithm can be viewed as a very effective meshless technique. It was already tested with success in the solution of plane elasticity problems, as shown in [20,18]. The method was recently applied with success to composite structures [25]. For the sake of completeness, some aspects related to the basic formulation will be described.

2. Interpolating wavelets

The Deslaurier–Dubuc fundamental function [21] of order $N = 2L + 1$ is defined as the autocorrelation of Daubechies scaling functions, ϕ_L [22], as follows:

$$\vartheta(x) = \int_{\mathbb{R}} \phi_L(y)\phi_L(y - x)dy \tag{1}$$

The scaling function ϕ_L satisfies the following properties:

1. $supp\,\phi_L = [0, 2L + 1]$;
2. $\phi_L \in W^{R/2,\infty}$ for some $R > 0$ (R is proportional to L): $|(d^s/dx^s)\phi_L| \leqslant C$, for all integers s, with com $0 \leqslant s \leqslant R/2$;
3. ϕ_L is orthogonal to all its integer translates: $\int \phi_L(x)\phi_L(x - k)dx = \delta_{0k}$;
4. All polynomials up to order L can be exactly represented as a linear combination of function ϕ_L and all its integer translates.

As a consequence of the above properties, function ϑ satisfies:

1. $supp\,\vartheta = [-N, N]$, and $\vartheta \in W^{R,\infty}$;
2. Due to the orthogonality of the translates of ϕ_L, the function ϑ presents the following interpolating property:

$$\vartheta(n) = \int_{\mathbb{R}} \phi_L(y)\phi_L(y - n)dy = \delta_{n0} \tag{2}$$

3. All polynomials up to order N can be exactly represented as a linear combination of function ϑ and all its integer translates.

* Corresponding author. Tel.: +351 218418253; fax: +351 218497650.
E-mail address: luis@civil.ist.utl.pt (L.M.S. Castro).

0263-8223/$ - see front matter © 2010 Elsevier Ltd. All rights reserved.
doi:10.1016/j.compstruct.2010.01.021

The plots of the function ϑ and its derivatives, for $N = 4$, are presented in Fig. 1.

Based on the fundamental function ϑ it is possible to build the complete wavelet system on $\mathbb{R}$. As described in detail in [17], tensor products will lead to wavelet systems on $\mathbb{R}^d$.

Following the ideas and techniques described in [23,24], it is possible to build a Deslaurier–Dubuc wavelet system *in the closed interval* [0,1]. As described in [20], we define for $j \geqslant j_0 = [\log_2(N/2)] + 1$

$$\vartheta_{jk} = \vartheta(2^j x - k) + \sum_{n=-N+1}^{-1} a_{nk}\vartheta(2^j x - n), \quad k = 0, \ldots, L \tag{3}$$

$$\vartheta_{jk} = \vartheta(2^j x - k), \quad k = L+1, \ldots, 2^j - L - 1, \tag{4}$$

$$\vartheta_{jk} = \vartheta(2^j x - k) + \sum_{n=2^j+1}^{2^j+N-1} b_{nk}\vartheta(2^j x - n), \quad k = 2^j - L, \ldots, 2^j, \tag{5}$$

where the coefficients a_{nk} and b_{nk} are defined by

$$a_{nk} = l^1_{jk}(n2^{-j}), \quad b_{nk} = l^2_{jk}(n2^{-j}) \tag{6}$$

and where l^1_{jk} and l^2_{jk} represent Lagrange interpolation polynomials of degree L, defined by

$$l^1_{jk} = \prod_{\substack{i=0 \\ i\neq k}}^{L} \frac{x - i2^{-j}}{k2^{-j} - i2^{-j}}, \quad l^2_{jk} = \prod_{\substack{i=2^j-L \\ i\neq k}}^{2^j} \frac{x - i2^{-j}}{k2^{-j} - i2^{-j}} \tag{7}$$

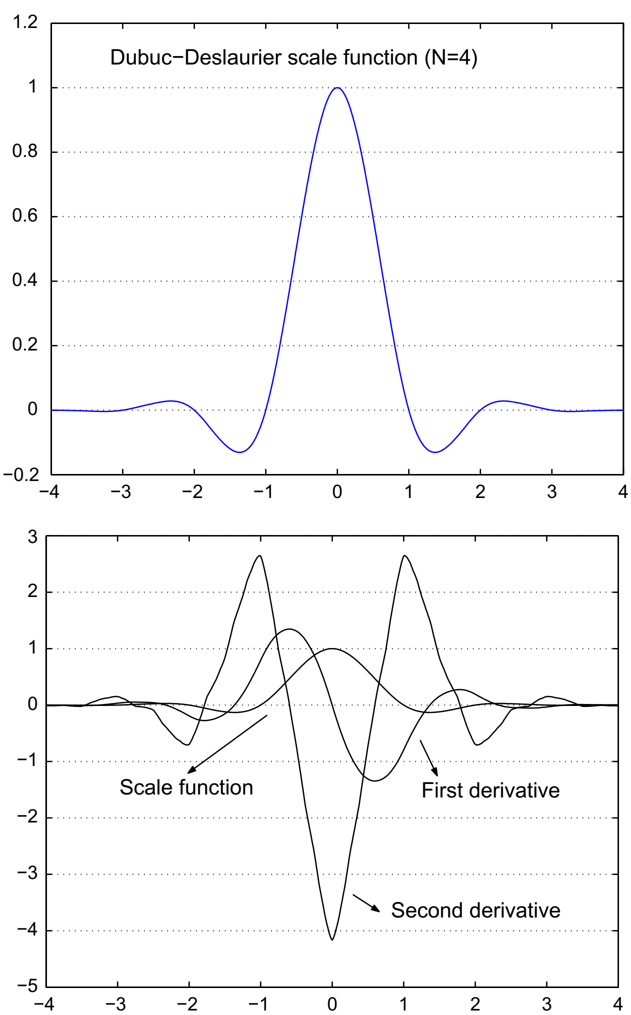

Fig. 1. Deslaurier–Dubuc function with $N = 4$ and its derivatives.

An interpolating multi-resolution analysis (MRA) in the interval [0,1] is defined by a set of closed subspaces $V_j = span\langle\vartheta_{jk}, k = 0, \ldots, 2^j\rangle \subset L^2(0,1)$. By using tensor products, it is then possible to define a multi-resolution on the square $[0,1]^2$. The two-dimensional scaling functions $\vartheta_{j,\boldsymbol{k}}, \boldsymbol{k} = (k_1,k_2) \in G_j = \{0,\ldots,2^j\}^2$ are defined by

$$\vartheta_{j,\boldsymbol{k}} = \vartheta_{jk_1} \otimes \vartheta_{jk_2} \tag{8}$$

The subspace $\mathbb{V}_j$ is the defined by:

$$\mathbb{V}_j = span\langle\vartheta_{j,\boldsymbol{k}}, \quad \boldsymbol{k} = (k_1,k_2) \in \{0,\ldots,2^j\}^2\rangle \tag{9}$$

It is easy to define an interpolation operator $L_j : C^0([0,1]^2) \to \mathbb{V}_j$

$$L_j f = \sum_{\boldsymbol{k}\in G_j} f(\boldsymbol{k}/2^j)\theta_{j,\boldsymbol{k}} \tag{10}$$

The wavelet basis for the complement space $\mathbb{W}_j = (L_{j+1} - L_j)\mathbb{V}_{j+1}$ is composed by the functions

$$\psi^{(1,0)}_{j,\boldsymbol{k}} = \vartheta_{j+1,2k_1-1} \otimes \vartheta_{j,2k_2} \tag{11}$$

$$\psi^{(0,1)}_{j,\boldsymbol{k}} = \vartheta_{j,2k_1} \otimes \vartheta_{j+1,2k_2-1} \tag{12}$$

$$\psi^{(1,1)}_{j,\boldsymbol{k}} = \vartheta_{j+1,2k_1-1} \otimes \vartheta_{j+1,2k_2-1} \tag{13}$$

and a hierarchical basis for $\mathbb{V}_j$ can be assembled as

$$\{\vartheta_{j_0,\boldsymbol{k}}, \boldsymbol{k} = (k_1,k_2) \in \{0,\ldots,2^{j_0}\}^2 \bigcup_{m=j_0}^{j-1} \left\{\psi^{(1,0)}_{m,\boldsymbol{k}}, \psi^{(0,1)}_{m,\boldsymbol{k}}, \psi^{(1,1)}_{m,\boldsymbol{k}}\right\},$$
$$\boldsymbol{k} = (k_1,k_2) \in \{0,\ldots,2^m\} \tag{14}$$

The grid points corresponding to the scaling functions and the wavelets are defined by

$$\zeta_{j,\boldsymbol{k}} = (k_1 2^{-j}, k_2 2^{-j}) \tag{15}$$

For the sake of simplicity we will use the following compact notation: given $\lambda = (\eta, j, \boldsymbol{k})$ with $\eta \in \Xi = \{0,1\}^2 \setminus \{0,0\}$, $j \geqslant j_0$, and $\boldsymbol{k}$ such that $\xi^\eta_{j,\boldsymbol{k}} \in [0,1]^2$, define

$$\psi_\lambda = \psi^\eta_{j,\boldsymbol{k}}, \quad \xi_\lambda = \xi^\eta_{j,\boldsymbol{k}} \tag{16}$$

Any continuous function $f \in C^0([0,1]^2)$ can be expanded in the form

$$f = \sum_{\boldsymbol{k}\in\{0,\ldots,2^{j_0}\}^2} \beta_{j_0\boldsymbol{k}}\vartheta_{j_0\boldsymbol{k}} + \sum_{\lambda\in\Lambda} \alpha_\lambda\psi_\lambda \tag{17}$$

where

$$\Lambda = \{(\eta, j, \boldsymbol{k}), \eta \in \Xi, j \geqslant j_0, \boldsymbol{k} \text{ such that } \xi^\eta_{j,\boldsymbol{k}} \in [0,1]^2\} \tag{18}$$

denotes the set of compact indexes.

It can be shown [20] that the scaling functions are responsible for representing f at a given level of resolution and the wavelets define the *detail* that is necessary to switch from one level of resolution to the next. Consequently, the value of the wavelet coefficients, α_λ, allow for the identification of the region of the domain where details are important – which correspond to the regions where the discretization should be improved.

3. Collocation technique

In this section we briefly describe the collocation method based on Deslaurier–Dubuc interpolating wavelets. We consider a uniform discretization, although the collocation method that we present here does not a priori require the uniformity of the grid and can easily be adapted to the case of non-uniform grids of dyadic points. For any $j \geqslant j_0$, let the dyadic grid G_j be defined by

$$G_j := \{\zeta_{j,\boldsymbol{k}}, \ \boldsymbol{k} \in \{0,\ldots,2^j\}^2\} \tag{19}$$

In order to take into account the boundary conditions, the grid G_j is subdivided into a set of interior nodes and sets of Neumann and Dirichlet boundary nodes. It is then possible to write:

$$G_j = G_j^{(i)} \cup G_j^{(N)} \cup G_j^{(D)}$$

with

$$G_j^{(i)} = G_j \cap [0,1]^2, \quad G_j^{(N)} = G_j \cap \Gamma_\sigma, \quad G_j^{(D)} = G_j \cap \Gamma_u$$

Problem (P) can be discretized as follows:
Find $\mathbf{u} \in \mathbb{V}_j$ such that

$$\mathcal{A}\mathbf{u}_h(p) = f(p) \quad \text{for all nodes } p \in G_j^{(i)} \tag{20}$$

$$\mathbf{u}_h(p) = g(\mathbf{x}_\lambda) \quad \text{for all nodes } p \in G_j^{(D)} \tag{21}$$

$$\mathcal{B}\mathbf{u}_h(p) = \mathbf{t}(p) \quad \text{for all nodes } p \in G_j^{(N)} \tag{22}$$

4. A layerwise theory

The layerwise proposed in this paper is based on the assumption of a first-order shear deformation theory [7] in each layer and the imposition of displacement continuity at layer's interfaces. In each layer the same assumptions as in the first-order plate theory are considered. Due to the size and complexity of the formulation we restrict the analysis to a three-layer laminate, as shown schematically in Fig. 2. However, the present approach is easily extendible for a general laminate.

The displacement field for the middle layer (sometimes known as the core of a sandwich laminate) is given as

$$u^{(2)}(x,y,z) = u_0(x,y) + z^{(2)}\theta_x^{(2)} \tag{23}$$

$$v^{(2)}(x,y,z) = v_0(x,y) + z^{(2)}\theta_y^{(2)} \tag{24}$$

$$w^{(2)}(x,y,z) = w_0(x,y) \tag{25}$$

where u and v are the in-plane displacements at any point (x,y,z), u_0 and v_0 denote the in-plane displacement of the point $(x,y,0)$ on the midplane, w is the transverse deflection, $\theta_x^{(2)}$ and $\theta_y^{(2)}$ are the rotations of the normals to the midplane about the y and x axes, respectively, for layer 2 (middle layer). The corresponding displacement field for the upper layer (3) and lower layer (1) are given, respectively, as

$$u^{(3)}(x,y,z) = u_0(x,y) + \frac{h_2}{2}\theta_x^{(2)} + \frac{h_3}{2}\theta_x^{(3)} + z^{(3)}\theta_x^{(3)} \tag{26}$$

$$v^{(3)}(x,y,z) = v_0(x,y) + \frac{h_2}{2}\theta_y^{(2)} + \frac{h_3}{2}\theta_y^{(3)} + z^{(3)}\theta_y^{(3)} \tag{27}$$

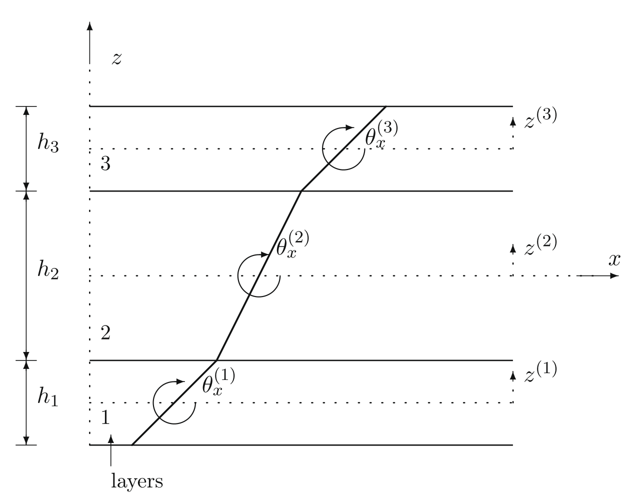

Fig. 2. 1D representation of the layerwise kinematics.

$$w^{(3)}(x,y,z) = w_0(x,y) \tag{28}$$

$$u^{(1)}(x,y,z) = u_0(x,y) - \frac{h_2}{2}\theta_x^{(2)} - \frac{h_1}{2}\theta_x^{(1)} + z^{(1)}\theta_x^{(1)} \tag{29}$$

$$v^{(1)}(x,y,z) = v_0(x,y) - \frac{h_2}{2}\theta_y^{(2)} - \frac{h_1}{2}\theta_y^{(1)} + z^{(1)}\theta_y^{(1)} \tag{30}$$

$$w^{(1)}(x,y,z) = w_0(x,y) \tag{31}$$

where h_k denotes the thickness of the kth layer and $z^{(k)} \in [-h_k/2, h_k/2]$ are the z-coordinates of the kth layer.

Strains of the kth layer are given by

$$\left\{\begin{matrix} \epsilon_{xx}^{(k)} \\ \epsilon_{yy}^{(k)} \\ \gamma_{xy}^{(k)} \\ \gamma_{xz}^{(k)} \\ \gamma_{yz}^{(k)} \end{matrix}\right\} = \left\{\begin{matrix} \frac{\partial u^{(k)}}{\partial x} \\ \frac{\partial v^{(k)}}{\partial y} \\ \frac{\partial u^{(k)}}{\partial y} + \frac{\partial v^{(k)}}{\partial x} \\ \frac{\partial u^{(k)}}{\partial z} + \frac{\partial w^{(k)}}{\partial x} \\ \frac{\partial v^{(k)}}{\partial z} + \frac{\partial w^{(k)}}{\partial y} \end{matrix}\right\} \tag{32}$$

Therefore, in-plane strains can be expressed as

$$\left\{\begin{matrix} \epsilon_{xx}^{(k)} \\ \epsilon_{yy}^{(k)} \\ \gamma_{xy}^{(k)} \end{matrix}\right\} = \left\{\begin{matrix} \epsilon_{xx}^{m(k)} \\ \epsilon_{yy}^{m(k)} \\ \gamma_{xy}^{m(k)} \end{matrix}\right\} + z^{(k)} \left\{\begin{matrix} \epsilon_{xx}^{f(k)} \\ \epsilon_{yy}^{f(k)} \\ \gamma_{xy}^{f(k)} \end{matrix}\right\} + \left\{\begin{matrix} \epsilon_{xx}^{mf(k)} \\ \epsilon_{yy}^{mf(k)} \\ \gamma_{xy}^{mf(k)} \end{matrix}\right\} \tag{33}$$

and the transverse shear strains as

$$\left\{\begin{matrix} \gamma_{xz}^{(k)} \\ \gamma_{yz}^{(k)} \end{matrix}\right\} = \left\{\begin{matrix} \frac{\partial w_0}{\partial x} + \theta_x^{(k)} \\ \frac{\partial w_0}{\partial y} + \theta_y^{(k)} \end{matrix}\right\} \tag{34}$$

The membrane strain components are given by

$$\left\{\begin{matrix} \epsilon_{xx}^{m(k)} \\ \epsilon_{yy}^{m(k)} \\ \gamma_{xy}^{m(k)} \end{matrix}\right\} = \left\{\begin{matrix} \frac{\partial u_0}{\partial x} \\ \frac{\partial v_0}{\partial y} \\ \frac{\partial u_0}{\partial y} + \frac{\partial v_0}{\partial x} \end{matrix}\right\} \tag{35}$$

The bending strains can be expressed as

$$\left\{\begin{matrix} \epsilon_{xx}^{f(k)} \\ \epsilon_{yy}^{f(k)} \\ \gamma_{xy}^{f(k)} \end{matrix}\right\} = \left\{\begin{matrix} \frac{\partial \theta_x^{(k)}}{\partial x} \\ \frac{\partial \theta_y^{(k)}}{\partial y} \\ \frac{\partial \theta_x^{(k)}}{\partial y} + \frac{\partial \theta_y^{(k)}}{\partial x} \end{matrix}\right\} \tag{36}$$

and the membrane-bending coupling components for layers 2, 3 and 1, are, respectively, given as

$$\left\{\begin{matrix} \epsilon_{xx}^{mf(2)} \\ \epsilon_{yy}^{mf(2)} \\ \gamma_{xy}^{mf(2)} \end{matrix}\right\} = \left\{\begin{matrix} 0 \\ 0 \\ 0 \end{matrix}\right\} \tag{37}$$

$$\left\{\begin{matrix} \epsilon_{xx}^{mf(3)} \\ \epsilon_{yy}^{mf(3)} \\ \gamma_{xy}^{mf(3)} \end{matrix}\right\} = \left\{\begin{matrix} \frac{h_2}{2}\frac{\partial \theta_x^{(2)}}{\partial x} + \frac{h_3}{2}\frac{\partial \theta_x^{(3)}}{\partial x} \\ \frac{h_2}{2}\frac{\partial \theta_y^{(2)}}{\partial y} + \frac{h_3}{2}\frac{\partial \theta_y^{(3)}}{\partial y} \\ \frac{h_2}{2}\left(\frac{\partial \theta_x^{(2)}}{\partial y} + \frac{\partial \theta_y^{(2)}}{\partial x}\right) + \frac{h_3}{2}\left(\frac{\partial \theta_x^{(3)}}{\partial y} + \frac{\partial \theta_y^{(3)}}{\partial x}\right) \end{matrix}\right\} \tag{38}$$

$$\left\{\begin{matrix} \epsilon_{xx}^{mf(1)} \\ \epsilon_{yy}^{mf(1)} \\ \gamma_{xy}^{mf(1)} \end{matrix}\right\} = \left\{\begin{matrix} -\frac{h_2}{2}\frac{\partial \theta_x^{(2)}}{\partial x} - \frac{h_1}{2}\frac{\partial \theta_x^{(1)}}{\partial x} \\ -\frac{h_2}{2}\frac{\partial \theta_y^{(2)}}{\partial y} - \frac{h_1}{2}\frac{\partial \theta_y^{(1)}}{\partial y} \\ -\frac{h_2}{2}\left(\frac{\partial \theta_x^{(2)}}{\partial y} + \frac{\partial \theta_y^{(2)}}{\partial x}\right) - \frac{h_1}{2}\left(\frac{\partial \theta_x^{(1)}}{\partial y} + \frac{\partial \theta_y^{(1)}}{\partial x}\right) \end{matrix}\right\} \tag{39}$$

Neglecting $\sigma_z^{(k)}$ for each orthotropic layer, the stress–strain relations in the fiber local coordinate system can be expressed as

$$\begin{Bmatrix} \sigma_1^{(k)} \\ \sigma_2^{(k)} \\ \tau_{12}^{(k)} \\ \tau_{23}^{(k)} \\ \tau_{31}^{(k)} \end{Bmatrix} = \begin{bmatrix} Q_{11} & Q_{12} & 0 & 0 & 0 \\ Q_{12} & Q_{22} & 0 & 0 & 0 \\ 0 & 0 & Q_{33} & 0 & 0 \\ 0 & 0 & 0 & Q_{44} & 0 \\ 0 & 0 & 0 & 0 & Q_{55} \end{bmatrix}^{(k)} \begin{Bmatrix} \varepsilon_1^{(k)} \\ \varepsilon_2^{(k)} \\ \gamma_{12}^{(k)} \\ \gamma_{23}^{(k)} \\ \gamma_{31}^{(k)} \end{Bmatrix} \tag{40}$$

where subscripts 1 and 2 denote, respectively, the fiber and the transverse to the fiber directions in the plane and 3 is the direction normal to the plate; the reduced stiffness components, $Q_{ij}^{(k)}$, are given by [7]

$$Q_{11}^{(k)} = \frac{E_1^{(k)}}{1-\nu_{12}^{(k)}\nu_{21}^{(k)}} \quad Q_{22}^{(k)} = \frac{E_2^{(k)}}{1-\nu_{12}^{(k)}\nu_{21}^{(k)}} \quad Q_{12}^{(k)} = \nu_{21}^{(k)} Q_{11}^{(k)}$$
$$Q_{33}^{(k)} = G_{12}^{(k)} \quad Q_{44}^{(k)} = G_{23}^{(k)} \quad Q_{55}^{(k)} = G_{31}^{(k)}$$
$$\nu_{21}^{(k)} = \nu_{12}^{(k)} \frac{E_2^{(k)}}{E_1^{(k)}}$$

in which $E_1^{(k)}, E_2^{(k)}, \nu_{12}^{(k)}, G_{12}^{(k)}, G_{23}^{(k)}$ and $G_{31}^{(k)}$ are material properties of the kth lamina.

By performing adequate coordinate transformation, the stress–strain relations in the global (x, y, z) coordinate system can be obtained as

$$\begin{Bmatrix} \sigma_{xx}^{(k)} \\ \sigma_{yy}^{(k)} \\ \tau_{xy}^{(k)} \\ \tau_{yz}^{(k)} \\ \tau_{zx}^{(k)} \end{Bmatrix} = \begin{bmatrix} \overline{Q}_{11}^{(k)} & \overline{Q}_{12}^{(k)} & \overline{Q}_{16}^{(k)} & 0 & 0 \\ \overline{Q}_{12}^{(k)} & \overline{Q}_{22}^{(k)} & \overline{Q}_{26}^{(k)} & 0 & 0 \\ \overline{Q}_{16}^{(k)} & \overline{Q}_{26}^{(k)} & \overline{Q}_{66}^{(k)} & 0 & 0 \\ 0 & 0 & 0 & \overline{Q}_{44}^{(k)} & \overline{Q}_{45}^{(k)} \\ 0 & 0 & 0 & \overline{Q}_{45}^{(k)} & \overline{Q}_{55}^{(k)} \end{bmatrix} \begin{Bmatrix} \varepsilon_{xx}^{(k)} \\ \varepsilon_{yy}^{(k)} \\ \gamma_{xy}^{(k)} \\ \gamma_{yz}^{(k)} \\ \gamma_{zx}^{(k)} \end{Bmatrix} \tag{41}$$

By considering α as the angle between x-axis and 1-axis, with 1-axis being the first principal material axis, connected usually with fiber direction, the components $\overline{Q}_{ij}^{(k)}$ can be calculated by adequate coordinate transformation, as in [7].

The equations of motion of this layerwise theory are derived from the dynamic version of the principle of virtual displacements. In the present work, only symmetric laminates are considered; therefore, the in-plane displacements u_0, v_0, which are uncoupled from the bending deformation, and related stress resultants can be discarded.

The virtual strain energy (δU), the virtual kinetic energy (δK) and the virtual work done by applied forces (δV), assuming a three-layer laminate, are given by

$$\begin{aligned} \delta U &= \int_{\Omega_0} \sum_{k=1}^{3} \left\{ \int_{-h_k/2}^{h_k/2} \left[\sigma_{xx}\left(z\delta\epsilon_{xx}^{f(k)} + \delta\epsilon_{xx}^{mf(k)}\right) + \sigma_{yy}\left(z\delta\epsilon_{yy}^{f(k)} + \delta\epsilon_{yy}^{mf(k)}\right) \right.\right. \\ &\quad \left.\left. + \tau_{xy}\left(z\delta\gamma_{xy}^{f(k)} + \delta\gamma_{xy}^{mf(k)}\right) + \tau_{xz}\delta\gamma_{xz}^{(k)} + \tau_{yz}\delta\gamma_{yz}^{(k)} \right] dz \right\} dx\,dy \\ &= \int_{\Omega_0} \sum_{k=1}^{3} \left(N_{xx}^{(k)}\delta\epsilon_{xx}^{mf(k)} + M_{xx}^{(k)}\delta\epsilon_{xx}^{f(k)} + N_{yy}^{(k)}\delta\epsilon_{yy}^{mf(k)} + M_{yy}^{(k)}\delta\epsilon_{yy}^{f(k)} \right. \\ &\quad \left. + N_{xy}^{(k)}\delta\gamma_{xy}^{mf(k)} + M_{xy}^{(k)}\delta\gamma_{xy}^{f(k)} + Q_x^{(k)}\delta\gamma_{xz}^{(k)} + Q_y^{(k)}\delta\gamma_{yz}^{(k)} \right) dx\,dy \end{aligned} \tag{42}$$

$$\delta K = \int_{\Omega_0} \sum_{k=1}^{3} \int_{-h_k/2}^{h_k/2} \rho^{(k)} (\dot{\mathbf{u}}^k \delta\dot{\mathbf{u}}^k + \dot{\mathbf{v}}^k \delta\dot{\mathbf{v}}^k + \dot{\mathbf{w}}^k \delta\dot{\mathbf{w}}^k)\, dz\,dx\,dy \tag{43}$$

and

$$\delta V = -\int_{\Omega_0} q\delta w_0\, dx\,dy \tag{44}$$

where Ω_0 denotes the midplane of the laminate, q is the external distributed load and

$$\begin{Bmatrix} N_{\alpha\beta}^{(k)} \\ M_{\alpha\beta}^{(k)} \end{Bmatrix} = \int_{-h_k/2}^{h_k/2} \sigma_{\alpha\beta}^{(k)} \begin{Bmatrix} 1 \\ z \end{Bmatrix} dz_k \tag{45}$$

$$Q_\alpha^{(k)} = \int_{-h_k/2}^{h_k/2} \tau_{\alpha z}^{(k)}\, dz_k \tag{46}$$

where α, β take the symbols x, y.

Substituting for $\delta U, \delta K, \delta V$, into the virtual work statement, noting that the virtual strains can be expressed in terms of the generalized displacements, integrating by parts to relieve from any derivatives of the generalized displacements and using the fundamental lemma of the calculus of variations, we obtain the equations of motion [7] with respect to seven degrees of freedom $\left(w_0, \theta_x^{(1)}, \theta_y^{(1)}, \theta_x^{(2)}, \theta_y^{(2)}, \theta_x^{(3)}, \theta_y^{(3)}\right)$ (see Fig. 2):

$$\delta w_0 : \sum_{k=1}^{3} \left(\frac{\partial Q_x^{(k)}}{\partial x} + \frac{\partial Q_y^{(k)}}{\partial y} \right) - q = \sum_{k=1}^{3} I_0^{(k)} \ddot{w}_0 \tag{47}$$

$$\begin{aligned} \delta\theta_x^{(1)} &: \frac{h_1}{2}\frac{\partial N_{xx}^{(1)}}{\partial x} - \frac{\partial M_{xx}^{(1)}}{\partial x} + \frac{h_1}{2}\frac{\partial N_{xy}^{(1)}}{\partial y} - \frac{\partial M_{xy}^{(1)}}{\partial y} + Q_x^{(1)} \\ &= I_0^{(1)}\left(\frac{h_1 h_2}{4}\ddot{\theta}_{x2} + \frac{h_1^2}{4}\ddot{\theta}_{x1}\right) + I_2^{(1)}\ddot{\theta}_{x1} \end{aligned} \tag{48}$$

$$\begin{aligned} \delta\theta_y^{(1)} &: \frac{h_1}{2}\frac{\partial N_{yy}^{(1)}}{\partial y} - \frac{\partial M_{yy}^{(1)}}{\partial y} + \frac{h_1}{2}\frac{\partial N_{xy}^{(1)}}{\partial x} - \frac{\partial M_{xy}^{(1)}}{\partial x} + Q_y^{(1)} \\ &= I_0^{(1)}\left(\frac{h_1 h_2}{4}\ddot{\theta}_{y2} + \frac{h_1^2}{4}\ddot{\theta}_{y1}\right) + I_2^{(1)}\ddot{\theta}_{y1} \end{aligned} \tag{49}$$

$$\begin{aligned} \delta\theta_x^{(2)} &: \frac{h_2}{2}\frac{\partial N_{xx}^{(1)}}{\partial x} - \frac{h_2}{2}\frac{\partial N_{xx}^{(3)}}{\partial x} - \frac{\partial M_{xx}^{(2)}}{\partial x} + \frac{h_2}{2}\frac{\partial N_{xy}^{(1)}}{\partial y} - \frac{h_2}{2}\frac{\partial N_{xy}^{(3)}}{\partial y} - \frac{\partial M_{xy}^{(2)}}{\partial y} + Q_x^{(2)} \\ &= I_0^{(1)}\left(\frac{h_2^2}{4}\ddot{\theta}_{x2} + \frac{h_1 h_2}{4}\ddot{\theta}_{x1}\right) + I_0^{(3)}\left(\frac{h_2^2}{4}\ddot{\theta}_{x2} + \frac{h_2 h_3}{4}\ddot{\theta}_{x3}\right) + I_2^{(2)}\ddot{\theta}_{x2} \end{aligned} \tag{50}$$

$$\begin{aligned} \delta\theta_y^{(2)} &: \frac{h_2}{2}\frac{\partial N_{yy}^{(1)}}{\partial y} - \frac{h_2}{2}\frac{\partial N_{yy}^{(3)}}{\partial y} - \frac{\partial M_{yy}^{(2)}}{\partial y} + \frac{h_2}{2}\frac{\partial N_{xy}^{(1)}}{\partial x} - \frac{h_2}{2}\frac{\partial N_{xy}^{(3)}}{\partial x} - \frac{\partial M_{xy}^{(2)}}{\partial x} + Q_y^{(2)} \\ &= I_0^{(1)}\left(\frac{h_2^2}{4}\ddot{\theta}_{y2} + \frac{h_1 h_2}{4}\ddot{\theta}_{y1}\right) + I_0^{(3)}\left(\frac{h_2^2}{4}\ddot{\theta}_{y2} + \frac{h_2 h_3}{4}\ddot{\theta}_{y3}\right) + I_2^{(2)}\ddot{\theta}_{y2} \end{aligned} \tag{51}$$

$$\begin{aligned} \delta\theta_x^{(3)} &: -\frac{h_3}{2}\frac{\partial N_{xx}^{(3)}}{\partial x} - \frac{\partial M_{xx}^{(3)}}{\partial x} - \frac{h_3}{2}\frac{\partial N_{xy}^{(3)}}{\partial y} - \frac{\partial M_{xy}^{(3)}}{\partial y} + Q_x^{(3)} \\ &= I_0^{(3)}\left(\frac{h_2 h_3}{4}\ddot{\theta}_{x2} + \frac{h_3^2}{4}\ddot{\theta}_{x3}\right) + I_2^{(3)}\ddot{\theta}_{x3} \end{aligned} \tag{52}$$

$$\begin{aligned} \delta\theta_y^{(3)} &: -\frac{h_3}{2}\frac{\partial N_{yy}^{(3)}}{\partial y} - \frac{\partial M_{yy}^{(3)}}{\partial y} - \frac{h_3}{2}\frac{\partial N_{xy}^{(3)}}{\partial x} - \frac{\partial M_{xy}^{(3)}}{\partial x} + Q_y^{(3)} \\ &= I_0^{(3)}\left(\frac{h_2 h_3}{4}\ddot{\theta}_{y2} + \frac{h_3^2}{4}\ddot{\theta}_{y3}\right) + I_2^{(3)}\ddot{\theta}_{y3} \end{aligned} \tag{53}$$

where

$$\left(I_0^{(k)}, I_2^{(k)}\right) = \int_{-h_k/2}^{h_k/2} \rho^{(k)}(1, z^2)\, dz \tag{54}$$

being ρ the specific mass of the material, and h_k the thickness of the kth layer.

The equations of motion can be written in terms of the displacements by substituting strains and stress resultants into previous equations. As an example the first equation is replaced by

$$\begin{aligned} \delta w_0 &: \sum_{k=1}^{3} h_k \left(\overline{Q}_{55}^{(k)} \left(\frac{\partial^2 w_0}{\partial x^2} + \frac{\partial \theta_x^{(k)}}{\partial x} \right) + \overline{Q}_{44}^{(k)} \left(\frac{\partial^2 w_0}{\partial y^2} + \frac{\partial \theta_y^{(k)}}{\partial y} \right) \right) - q \\ &= \sum_{k=1}^{3} I_0^{(k)} \ddot{w}_0 \end{aligned} \tag{55}$$

5. Interpolation of differential equations of motion and boundary conditions by wavelets

The equations of motion are now interpolated by wavelets, for each node i. For example, Eq. (55) is then expressed as

$$\delta w_0 : \sum_{k=1}^{3} h_k \left(\overline{Q}_{55}^{(k)} \left(\sum_{j=1}^{N} a_j^w \frac{\partial^2 \varphi_j}{\partial x^2} + \sum_{j=1}^{N} a_j^{\theta_x^{(k)}} \frac{\partial \varphi_j}{\partial x} \right) + \overline{Q}_{44}^{(k)} \left(\sum_{j=1}^{N} a_j^w \frac{\partial^2 \varphi_j}{\partial y^2} + \sum_{j=1}^{N} a_j^{\theta_y^{(k)}} \frac{\partial \varphi_j}{\partial y} \right) \right) - q = - \sum_{k=1}^{3} I_0^{(k)} \omega^2 \sum_{j=1}^{N} a_j^w \varphi_j \quad (56)$$

where φ_j was defined before and N represents the total number of discretization points. The other six equations are interpolated in a similar way. The vector of unknowns is now composed of the interpolation parameters a_j, for $w_0, \theta_x^{(1)}, \theta_y^{(1)}, \theta_x^{(2)}, \theta_y^{(2)}, \theta_x^{(3)}, \theta_y^{(3)}$, respectively.

For each boundary node, the wavelet interpolation is also quite simple. As an example, a simply-supported condition on the $x = \beta$ edge with outward normal direction α imposes seven boundary conditions, as follows:

$$w_0 = 0 \quad (57)$$

$$M_{\alpha\alpha}^{(k)} = 0 \quad (58)$$

$$\theta_{\beta}^{(k)} = 0 \quad (59)$$

These conditions are equivalent to

$$w_0 = 0 \quad (60)$$

$$\delta\theta_x^{(1)} \left(-\frac{h_1}{2} N_{xx}^{(1)} - \frac{h_1}{2} N_{xy}^{(1)} + M_{xx}^{(1)} \right) + \delta\theta_x^{(2)} \left(-\frac{h_2}{2} N_{xx}^{(1)} + \frac{h_2}{2} N_{xx}^{(3)} - \frac{h_2}{2} N_{xy}^{(1)} + \frac{h_2}{2} N_{xy}^{(3)} + M_{xx}^{(2)} \right) + \delta\theta_x^{(3)} \left(\frac{h_3}{2} N_{xx}^{(3)} + M_{xx}^{(3)} \right) = 0 \quad (61)$$

$$\theta_{\beta}^{(k)} = 0 \quad (62)$$

The interpolation of boundary equations leads to a change in the global equations system. For each node i were the equations are valid, the following equations are imposed. For example, Eq. (60) is interpolated as

$$\sum_{j=1}^{N} a_j^w \varphi_i = 0 \quad (63)$$

where N represents the total number of grid points. The other boundary conditions are interpolated in the same way.

6. Numerical examples

Two numerical examples are considered. In both a regular grid was used.

6.1. Three layer square sandwich plate in bending, under uniform load

A simply-supported sandwich plate under uniformly distributed load (q) is considered. This is the classical sandwich plate example of Srinivas [27]. The plate thickness is $h = 0.1$. The thickness of three layers are $h_1/h = h_3/h = 0.1; h_2/h = 0.8$. The plate side is $a = 1$. The material properties of the sandwich core are expressed in the stiffness matrix, $\overline{Q}_{core}$ as:

$$\overline{Q}_{core} = \begin{bmatrix} 0.999781 & 0.231192 & 0 & 0 & 0 \\ 0.231192 & 0.524886 & 0 & 0 & 0 \\ 0 & 0 & 0.262931 & 0 & 0 \\ 0 & 0 & 0 & 0.266810 & 0 \\ 0 & 0 & 0 & 0 & 0.159914 \end{bmatrix}$$

Skins material properties are related with core properties by a factor R as

$$\overline{Q}_{skin} = R\overline{Q}_{core}$$

Transverse displacement and stresses are normalized through factors

$$\bar{w} = w(a/2, a/2, 0)\frac{0.999781}{hq}$$

$$\bar{\sigma}_x^1 = \frac{\sigma_x^{(1)}(a/2, a/2, -h/2)}{q}; \quad \bar{\sigma}_x^2 = \frac{\sigma_x^{(1)}(a/2, a/2, -2h/5)}{q};$$

$$\bar{\sigma}_x^3 = \frac{\sigma_x^{(2)}(a/2, a/2, -2h/5)}{q}$$

$$\bar{\sigma}_y^1 = \frac{\sigma_y^{(1)}(a/2, a/2, -h/2)}{q}; \quad \bar{\sigma}_y^2 = \frac{\sigma_y^{(1)}(a/2, a/2, -2h/5)}{q};$$

$$\bar{\sigma}_y^3 = \frac{\sigma_y^{(2)}(a/2, a/2, -2h/5)}{q}$$

$$\bar{\tau}_{xz}^1 = \frac{\tau_{xz}^{(2)}(0, a/2, 0)}{q}; \quad \bar{\tau}_{xz}^2 = \frac{\tau_{xz}^{(2)}(0, a/2, -2h/5)}{q}$$

Transverse displacement and stresses for a sandwich plate are indicated in Tables 1–3 and compared with various formulations. The transverse shear stresses are obtained directly from the constitutive equations, at each layer's middle surface. These formulations provide very good results both for displacement and stresses. It can be seen that the present formulation achieves very good results for all cases, without the use of shear correction factors. The FSDT and HSDT results of Pandya [28] cannot match our formulation for

Table 1
Square laminated plate under uniform load – $R = 5$.

Method	$\bar{w}$	$\bar{\sigma}_x^1$	$\bar{\sigma}_x^2$	$\bar{\sigma}_x^3$	$\bar{\sigma}_y^1$	$\bar{\sigma}_y^2$	$\bar{\sigma}_y^3$	$\bar{\tau}_{xz}^1$	$\bar{\tau}_{xz}^2$
HSDT [28]	256.13	62.38	46.91	9.382	38.93	30.33	6.065	3.089	2.566
FSDT [28]	236.10	61.87	49.50	9.899	36.65	29.32	5.864	3.313	2.444
CLT	216.94	61.141	48.623	9.783	36.622	29.297	5.860	4.5899	3.386
Ferreira [26]	258.74	59.21	45.61	9.122	37.88	29.59	5.918	3.593	3.593
Ferreira ($N = 15$) [8]	257.38	58.725	46.980	9.396	37.643	27.714	4.906	3.848	2.839
Exact [27]	258.97	60.353	46.623	9.340	38.491	30.097	6.161	4.3641	3.2675
HSDT [15] ($N = 11$)	253.6710	59.6447	46.4292	9.2858	38.0694	29.9313	5.9863	3.8449	1.9650
HSDT [15] ($N = 15$)	256.2387	60.1834	46.8581	9.3716	38.3592	30.1642	6.0328	4.2768	2.2227
HSDT [15] ($N = 21$)	257.1100	60.3660	47.0028	9.4006	38.4563	30.2420	6.0484	4.5481	2.3910
Present (9×9 grid)	62.2204	14.2841	10.4158	2.0832	13.7422	10.4223	2.0845	1.6244	−20.7302
Present (17×17 grid)	257.5719	59.9865	46.3043	9.2609	38.3217	29.9783	5.9957	4.0404	2.5236
Present (33×33 grid)	258.0558	60.0714	46.3719	9.2744	38.3745	30.0205	6.0041	4.0855	2.1780

Table 2
Square laminated plate under uniform load – $R = 10$.

Method	$\bar{w}$	$\bar{\sigma}_x^1$	$\bar{\sigma}_x^2$	$\bar{\sigma}_x^3$	$\bar{\sigma}_y^1$	$\bar{\sigma}_y^2$	$\bar{\sigma}_y^3$	$\bar{\tau}_{xz}^1$	$\bar{\tau}_{xz}^2$
HSDT [28]	152.33	64.65	51.31	5.131	42.83	33.97	3.397	3.147	2.587
FSDT [28]	131.095	67.80	54.24	4.424	40.10	32.08	3.208	3.152	2.676
CLT	118.87	65.332	48.857	5.356	40.099	32.079	3.208	4.3666	3.7075
Ferreira [26]	159.402	64.16	47.72	4.772	42.970	42.900	3.290	3.518	3.518
Ferreira ($N = 15$) [8]	158.55	62.723	50.16	5.01	42.565	34.052	3.400	3.596	3.053
Exact [27]	159.38	65.332	48.857	4.903	43.566	33.413	3.500	4.0959	3.5154
Third-order [15] ($N = 11$)	153.0084	64.7415	49.4716	4.9472	42.8860	33.3524	3.3352	2.7780	1.8207
Third-order [15] ($N = 15$)	154.2490	65.2223	49.8488	4.9849	43.1521	33.5663	3.3566	3.1925	2.1360
Third-order [15] ($N = 21$)	154.6581	65.3809	49.9729	4.9973	43.2401	33.6366	3.3637	3.5280	2.3984
Present (9×9 grid)	57.4138	15.1284	10.1106	1.0111	16.9339	12.3352	1.2335	4.3155	−29.3453
Present (17×17 grid)	158.2166	64.8058	48.4108	4.8411	43.3641	33.2844	3.3284	3.9014	3.1020
Present (33×33 grid)	158.7656	64.9739	48.5442	4.8544	43.4739	33.3722	3.3372	3.9665	2.5452

Table 3
Square laminated plate under uniform load – $R = 15$.

Method	$\bar{w}$	$\bar{\sigma}_x^1$	$\bar{\sigma}_x^2$	$\bar{\sigma}_x^3$	$\bar{\sigma}_y^1$	$\bar{\sigma}_y^2$	$\bar{\sigma}_y^3$	$\bar{\tau}_{xz}^1$	$\bar{\tau}_{xz}^2$
HSDT [28]	110.43	66.62	51.97	3.465	44.92	35.41	2.361	3.035	2.691
FSDT [28]	90.85	70.04	56.03	3.753	41.39	33.11	2.208	3.091	2.764
CLT	81.768	69.135	55.308	3.687	41.410	33.128	2.209	4.2825	3.8287
Ferreira [26]	121.821	65.650	47.09	3.140	45.850	34.420	2.294	3.466	3.466
Ferreira ($N = 15$) [8]	121.184	63.214	50.571	3.371	45.055	36.044	2.400	3.466	3.099
Exact [27]	121.72	66.787	48.299	3.238	46.424	34.955	2.494	3.9638	3.5768
Third-order [15] ($N = 11$)	113.5941	66.3646	49.8957	3.3264	45.2979	34.9096	2.3273	2.1686	1.5578
Third-order [15] ($N = 15$)	114.3874	66.7830	50.2175	3.3478	45.5427	35.1057	2.3404	2.6115	1.9271
Third-order [15] ($N = 21$)	114.6442	66.9196	50.3230	3.3549	45.6229	35.1696	2.3446	3.0213	2.2750
Present (9×9 grid)	61.4771	12.4621	5.3235	0.3549	96.9302	69.2177	4.6145	8.5351	−50.4572
Present (17×17 grid)	120.6174	66.1364	47.7599	3.1840	46.1655	34.7910	2.3194	3.8100	3.4344
Present (33×33 grid)	121.1937	66.3714	47.9463	3.1964	46.3274	34.9210	2.3281	3.8865	2.7341

Table 4
[0°/90°/90°/0°] square laminated plate under sinusoidal load.

$\frac{a}{h}$	Method	$\bar{w}$	$\bar{\sigma}_{xx}$	$\bar{\sigma}_{yy}$	$\bar{\tau}_{zx}$	$\bar{\tau}_{xy}$
4	HSDT [29]	1.8939	0.6806	0.6463	0.2109	0.0450
	HSDT [31]	1.8937	0.6651	0.6322	0.2064	0.0440
	FSDT [30]	1.7100	0.4059	0.5765	0.1398	0.0308
	Elasticity [32]	1.954	0.720	0.666	0.270	0.0467
	Ferreira et al. [15] ($N = 21$)	1.8864	0.6659	0.6313	0.1352	0.0433
	Ferreira (layerwise) [12] ($N = 21$)	1.9075	0.6432	0.6228	0.2166	0.0441
	Present (17×17 grid)	1.9091	0.6429	0.6265	0.2173	0.0442
	Present (33×33 grid)	1.9091	0.6429	0.6265	0.2173	0.0443
10	HSDT [29]	0.7149	0.5589	0.3974	0.2697	0.0273
	HSDT [31]	0.7147	0.5456	0.3888	0.2640	0.0268
	FSDT [30]	0.6628	0.4989	0.3615	0.1667	0.0241
	Elasticity [32]	0.743	0.559	0.403	0.301	0.0276
	Ferreira et al. [15] ($N = 21$)	0.7153	0.5466	0.4383	0.3347	0.0267
	Ferreira (layerwise) [12] ($N = 21$)	0.7309	0.5496	0.3956	0.2888	0.0273
	Present (17×17 grid)	0.7303	0.5487	0.3966	0.2993	0.0273
	Present (33×33 grid)	0.7303	0.5487	0.3966	0.2993	0.0273
20	HSDT [29]	0.5061	0.5523	0.3110	0.2883	0.0233
	HSDT [31]	0.5060	0.5393	0.3043	0.2825	0.0228
	FSDT [30]	0.4912	0.5273	0.2957	0.1749	0.0221
	Elasticity [32]	0.517	0.543	0.309	0.328	0.0230
	Ferreira (layerwise) [12] ($N = 21$)	0.5121	0.5417	0.3056	0.3248	0.0230
	Ferreira et al. [15] ($N = 21$)	0.5070	0.5405	0.3648	0.3818	0.0228
	Present (17×17 grid)	0.5113	0.5407	0.3073	0.3256	0.0230
	Present (33×33 grid)	0.5113	0.5407	0.3073	0.3256	0.0230
100	3strip[29]	0.4343	0.5507	0.2769	0.2948	0.0217
	HSDT [31]	0.4343	0.5387	0.2708	0.2897	0.0213
	FSDT [30]	0.4337	0.5382	0.2705	0.1780	0.0213
	Elasticity [32]	0.4347	0.539	0.271	0.339	0.0214
	Ferreira et al. [15] ($N = 21$)	0.4365	0.5413	0.3359	0.4106	0.0215
	Ferreira (layerwise) [12] ($N = 21$)	0.4374	0.5420	0.2697	0.3232	0.0216
	Present (17×17 grid)	0.4347	0.5389	0.2710	0.3358	0.0214
	Present (33×33 grid)	0.4348	0.5391	0.2711	0.3359	0.0214

sandwich laminates where skin properties are quite different than core properties, which is the typical industrial case. Therefore, for $R \geqslant 15$, this formulation should be adopted. The work of one of the authors in laminated shell finite elements [26] and multiquadrics [8] using a first order shear deformation approach is also compared. The results are as good or better than the present formulation. However, this was achieved by a shear correction procedure [8] that is dependent on some assumptions that may not be general, although quite good for all tested cases so far. The present layerwise formulation is better than the third-order formulation presented by Ferreira et al. [15], particularly in sandwich plates with skin properties much higher than core properties.

6.2. Four layer (0/90/90/0) square cross-ply laminated plate under sinusoidal load

A simply supported square laminated plate of side a and thickness h is composed of four equally layers oriented at [0°/90°/90°/0°]. The plate is subjected to a sinusoidal vertical pressure of the form

$$p_z = P \sin\left(\frac{\pi x}{a}\right) \sin\left(\frac{\pi y}{a}\right)$$

with the origin of the coordinate system located at the lower left corner on the midplane.

The orthotropic material properties are given by

$$E_1 = 25.0E_2 \quad G_{12} = G_{13} = 0.5E_2 \quad G_{23} = 0.2E_2 \quad \nu_{12} = 0.25$$

In Table 4 the present method is compared with a finite strip formulation by Akhras [29,30] who used three strips, an analytical solution by Reddy [7,31] using a higher-order formulation and an exact three dimensional solution by Pagano [32]. The present solution is also compared with another higher-order solution by the authors [15]. The in-plane displacements, the transverse displacements, the normal stresses and the in-plane and transverse shear stresses are presented in normalized form as

$$\bar{w} = \frac{10^2 w_{max} h^3 E_2}{Pa^4} \quad \bar{\sigma}_{xx} = \frac{\sigma_{xx} h^2}{Pa^2} \quad \bar{\sigma}_{yy} = \frac{\sigma_{yy} h^2}{Pa^2} \quad \bar{\tau}_{zx} = \frac{\tau_{zx} h}{Pa}$$

$$\bar{\tau}_{xy} = \frac{\tau_{xy} h^2}{Pa^2}$$

The transverse shear stresses are calculated directly from the constitutive equations. This is a feature of this theory, whereas other equivalent single layer theories such as Reddy's third order theory [7,31] one may calculate transverse shear stresses using the equilibrium equations. The present layerwise theory discretized with wavelets presents better results than previous results by Ferreira et al. [15]. Results for transverse displacements and stresses are better than Akhras and Reddy when referred to the exact solutions.

7. Conclusions

The first-order and the third-order shear deformation theories are equivalent single-layer theories, with laminate degrees of freedom, where all layers have the same rotations. Layerwise formulations can accommodate better kinematics of some laminates, particularly the sandwich laminates, where core and skin materials are of different stiffness.

In this paper the static analysis of sandwich plates by the use of a wavelet collocation technique, and using a layerwise theory with independent rotations in each layer is performed here for the first time. The equations of motion were derived and interpolated. Boundary conditions interpolation was schematically formulated. Composite laminated plate and sandwich plate were considered for testing of the present methodology and results obtained showed excellent accuracy for all cases. The method produces highly accurate results for isotropic, laminated composites and sandwich plates.

References

[1] Laura PAA, Gutierrez RH. Analysis of vibrating Timoshenko beams using the method of differential quadrature. Shock Vib 1993;1(1):89–93.
[2] Bert CW, Malik M. Differential quadrature method in computational mechanics: a review. Appl Mech Rev 1996;49(1):1–28.
[3] Liew KM, Han JB, Xiao ZM. Vibration analysis of circular Mindlin plates using differential quadrature method. J Sound Vib 1997;205(5):617–30.
[4] Bathe K. Finite element procedures. Englewood Cliffs (NJ): Prentice-Hall; 1996.
[5] Weaver W, Johnson P. Structural dynamics by finite elements. Englewood Cliffs (NJ); 1987.
[6] Reddy JN. Introduction to the finite element method. 3rd ed. New York: McGraw-Hill; 2006.
[7] Reddy JN. Mechanics of laminated composite plates and shells. 2nd ed. New York: CRC Press; 2004.
[8] Ferreira AJM. A formulation of the multiquadric radial basis function method for the analysis of laminated composite plates. Compos Struct 2003;59:385–92.
[9] Ferreira AJM. Thick composite beam analysis using a global meshless approximation based on radial basis functions. Mech Adv Mater Struct 2003;10:271–84.
[10] Ferreira AJM. Free vibration analysis of Timoshenko beams and Mindlin plates by radial basis functions. Int J Comput Methods 2005;2(1):15–31.
[11] Ferreira AJM. Polyharmonic (thin-plate) splines in the analysis of composite plates. Int J Mech Sci 2005;46:1549–69.
[12] Ferreira AJM. Analysis of composite plates using a layerwise deformation theory and multiquadrics discretization. Mech Adv Mater Struct 2005;12(2):99–112.
[13] Ferreira AJM, Batra RC, Roque CMC, Qian LF, Martins PALS. Static analysis of functionally graded plates using third-order shear deformation theory and a meshless method. Compos Struct 2005;69:449–57.
[14] Ferreira AJM, Fasshauer GE. Natural frequencies of shear deformable beams and plates by a RBF-pseudospectral method. Comput Methods Appl Mech Eng 2006;196:134–46.
[15] Ferreira AJM, Roque CMC, Martins PALS. Analysis of composite plates using higher-order shear deformation theory and a finite point formulation based on the multiquadric radial basis function method. Composites: Part B 2003;34:627–36.
[16] Ferreira AJM, Roque CMC, Martins PALS. Radial basis functions and higher-order theories in the analysis of laminated composite beams and plates. Compos Struct 2004;66:287–93.
[17] Bertoluzza S. An adaptive collocation method based on interpolating wavelets, in multiscale wavelet methods for partial differential equations. In: Dahmen, Kurdila, Oswald, Academic Press; 1997.
[18] Castro LMS, Bertoluzza S. Técnicas de colocação baseadas em sistemas de wavelets na resolução de problemas de elasticidade, Metodos Numericos en Ingenieria V, SEMNI; 2002.
[19] Bertoluzza S, Naldi G. A Wavelet collocation method for the numerical solution of partial differential equations. Appl Comput Harm Anal 1996;3:1–9.
[20] Bertoluzza S, Castro LM. Adaptive wavelet collocation for elasticity: first results. Pavia, Italy: IAN–CNR; 2001 [preprint].
[21] Deslaurier G, Dubuc S. Symmetric iterative interpolation processes. Constr Approx 1989;5.
[22] Daubechies I. Orthonormal bases of compactly supported wavelets. Commun Pure Appl Math 1988;41:909–96.
[23] Donoho D. Interpolating wavelet transform. Department of Statistics, Stanford University; 1992 [preprint].
[24] Cohen A, Daubechies I, Vial P. Wavelets on the interval and fast wavelet transforms. ACHA 1993;1:54–81.
[25] Ferreira AJM, Castro L MS, Bertoluzza S. A high order collocation method for the static and vibration analysis of composite plates using a first-order theory. Compos Struct 2009;89:424–32.
[26] Ferreira AJM, Barbosa JT. Buckling behaviour of composite shells. Compos Struct 2000;50:93–8.
[27] Srinivas S. A refined analysis of composite laminates. J Sound Vib 1973;30:495–507.
[28] Pandya BN, Kant T. Higher-order shear deformable theories for flexure of sandwich plates – finite element evaluations. Int J Solids Struct 1988;24:419–51.
[29] Akhras G, Cheung MS, Li W. Finite strip analysis for anisotropic laminated composite plates using higher-order deformation theory. Comput Struct 1994;52(3):471–7.
[30] Akhras G, Cheung MS, Li W. Static and vibrations analysis of anisotropic laminated plates by finite strip method. Int J Solids Struct 1993;30(22):3129–37.
[31] Reddy JN. A simple higher-order theory for laminated composite plates. J Appl Mech 1984;51:745–52.
[32] Pagano NJ. Exact solutions for rectangular bidirectional composites and sandwich plates. J Compos Mater 1970;4:20–34.